Chapter 4 –
MINERAL CHEMISTRY

4.1 Results

Mineral compositions were obtained by electron microprobe at the "Istituto di Geologia Ambientale e Geoingegnereia" (IGAG)-CNR, Rome, and by SEM-EDS analyses at the "Dipartimento di Scienze Geologiche", University of Catania.
Tables and analytical procedures are reported in Appendix 2 and 3, respectively.

4.1.1Pyroxene

Pyroxene analyses are recalculated using the scheme of Yoder and Tilley (*1962*). The pyroxene formula unit is normalized to 6 oxygens and recalculated to 4 cations. Fe^{+2}/Fe^{+3} partitioning is according to Papike et al. (1974). The cations are allocated to their structural sites according to the IMA guidelines. Pyroxene end-members are recalculated using the method of Cawthorn and Collerson (*1974*).
Analyses are reported in Appendix 2 - Table 2.1. Nomenclature is according to Morimoto (*1988*).

Clinopyroxene represents the most abundant phenocryst phase in the basaltic lithotypes of Serre (LMA, F and A samples) and Leonforte (VG samples). It occurs fresh or completely replaced by chlorite and/or actinolite. Micro-analyses performed on the relatively fresh clinopyroxene of LMA, A and VG samples have provided reliable compositional data. On the contrary, in the F samples, clinopyroxene is preserved from pervasive chlorite and/or actinolite alteration only in rare and tiny crystal portions. As a consequence analyses can be hardly considered clean and reliable and have been therefore rejected.

In this chapter, a first classification of pyroxene is made using the diagrams proposed by Leterrier et al. (*1982*, Fig. 4.1), that are useful tools to discriminate between clinopyroxene deriving from magmas of different geochemical affinities. Indeed, clinopyroxene of alkaline basalts are usually characterized by higher Ca, Ti and Na contents than clinopyroxene deriving from basalts of different affinities. The same occurs for Cr contents that can reach high values in clinopyroxene of intra-plate

tholeiites and in alkali basalts, whereas in orogenic ones it remains always low (*Leterrier et al., 1982*).

In these diagrams, a calc-alkaline affinity is clearly indicated for the clinopyroxene from the Serre dykes (LMA and A samples). Conversely, compositions of the clinopyroxene from the Leonforte sill (VG samples; fig. 4.1c), plot mostly as non-alkali basalts, possibly as a result of post-magmatic loss of Ca and/or Na, which probably affected also part of the A samples.

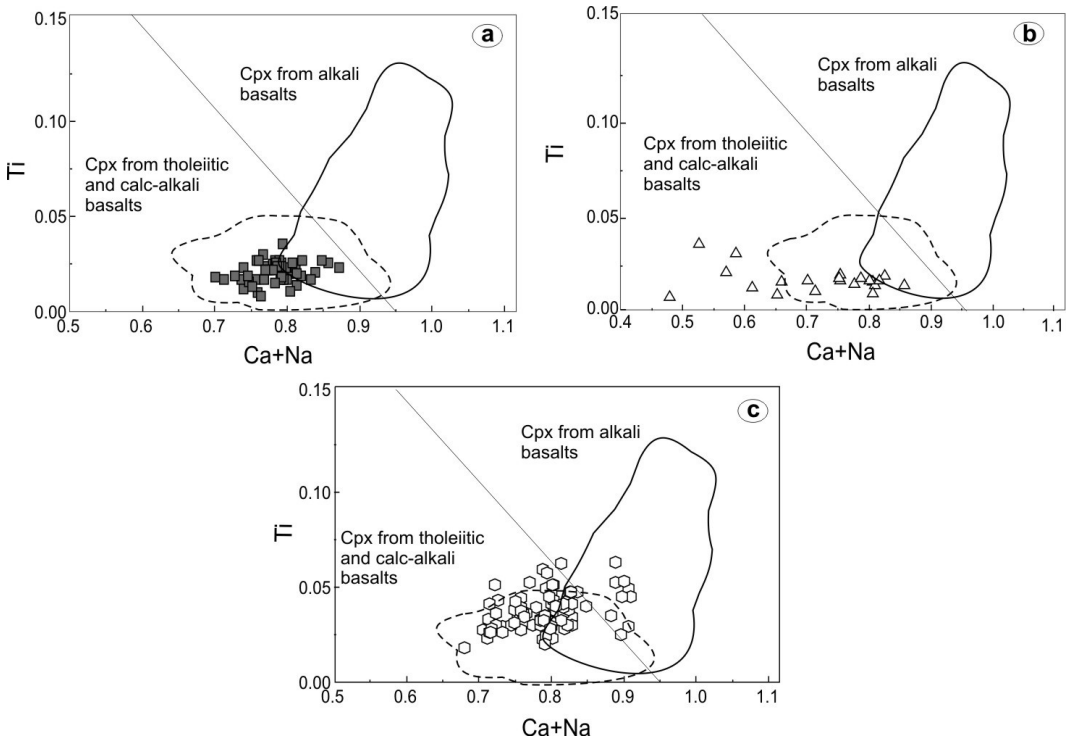

Fig. 4.1: Discrimination diagrams Ti (pfu) vs. Ca+Na (pfu) for clinopyroxene of **a)** LMA samples; **b)** A samples; **c)** VG samples. Solid and dashed line: cpx composition of alkali and non-alkali basalts, respectively, after Leterrrier et al. (*1982*).

In all the analyzed crystals, clinopyroxene shows an augitic composition (Fig. 4.2). However, in the Wo-En-Fs diagram, some phenocrysts from the A samples and numerous from VG samples fall in the Diopside field (Fig. 4.2b, c).

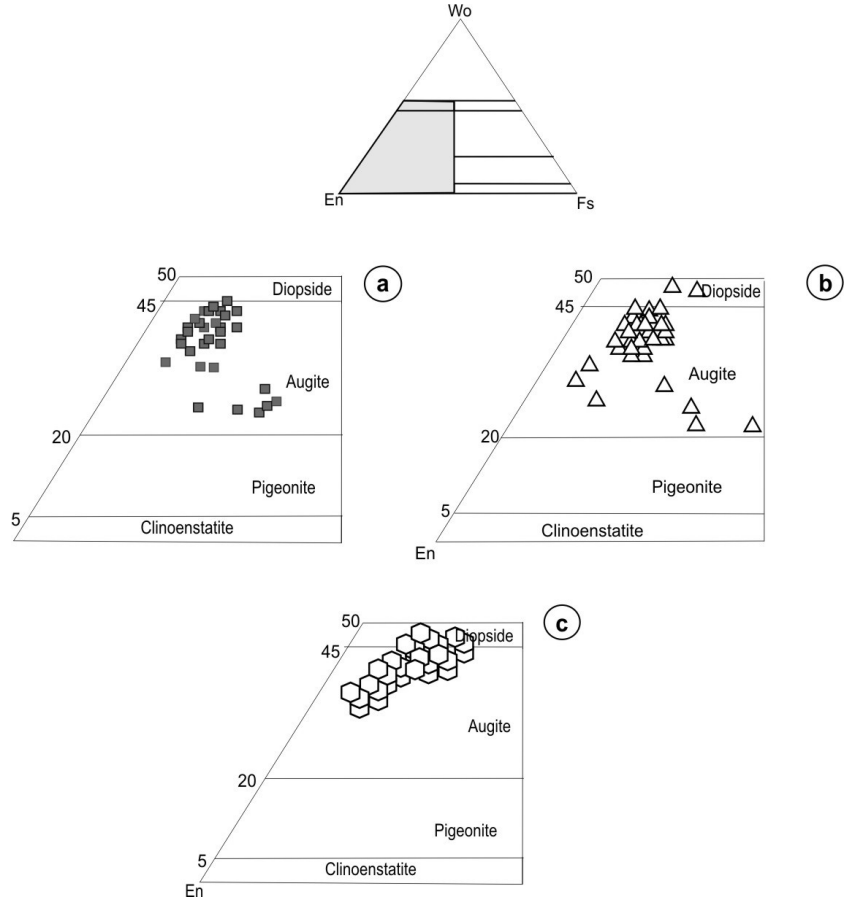

Fig. 4.2: Wo-En-Fs classification diagram (*Morimoto, 1988*) for clinopyroxene from **a)** LMA dykes; **b)** A dykes; **c)** VG dykes.

Specific information on the pyroxene from the different groups of samples is reported as follows.

Calabrian dykes

Mammola – Piani di Limina (LMA samples)

Clinopyroxene is augite ($Wo_{24.4-43.5}$ - $En_{46.9-59.4}$ - $Fs_{7.8-25.7}$; Fig. 4.3a), characterized by high MgO (15.5 – 20.3 wt%) and CaO contents (10.6 – 21.4 wt%), variable contents of FeO (3.3 – 14.4 wt%), low TiO_2 (0.42 – 1.25 wt%), typical of calcalkaline rocks (fig. 4.1), and very low contents of Cr_2O_3 (avg 0.46 wt%). Al_2O_3 is in the range of 1.5 – 5.0 wt. % and Na_2O shows values up to 1.2 wt. %.MnO usually lacks or shows very low contents (up to 0.26 wt. %).

Mg# [$Mg/(Mg+Fe^{2+})$] ranges between 66 and 87.

From core to rim of phenocrysts, it is occasionally possible to detect a preponderant normal compositional zoning reflected in the FeO and TiO_2 slight increase, and MgO and Al_2O_3 decrease.

Antonimina (A samples)

In group A samples, clinopyroxene is mainly represented by augite (Wo_{22-48}-En_{37-64}-Fs_{5-36}) and by crystals that, in the Wo-En-Fs diagram, fall in the diopside field (Fig. 4.3b). They all have high MgO (11.0 - 19.9 wt.%) and CaO contents (10.4 - 21.3 wt.%) and strongly variable Al_2O_3 (1.3 - 7.4 wt. %) and FeO (2.9 and 13.6 wt.%) contents. TiO_2 and Na_2O show low contents (0.2 – 1.0 wt.%; 0.0 – 1.7 wt.%, respectively). MnO and Cr_2O_3 usually have very low contents (0.08 - 0.35 wt. % and up to 0.42 wt. %, respectively).

Mg# value ranges between 69 and 88.

Zoned crystals are rare or not observable optically. However, from core to rim, occasionally an increase in FeO, and a decrease in MgO, TiO_2 and Al_2O_3 have been detected, defining a normal compositional zoning

Sicilian dykes

Leonforte (VG samples)

Clinopyroxene mainly has an augitic – diopsidic composition ($Wo_{35.8-46.2}$ - $En_{35.8-56.8}$ - $Fs_{6.9-17.1}$) characterized by variable contents in CaO (16.4 – 22.2 wt%), Al_2O_3 (1.9 – 6.5 wt%), Na_2O (0.3 – 1.6 wt%) and TiO_2 (0.7 – 2.2 wt%).

Rarely and only in some Mg-rich crystals, little amounts of Cr have been detected (Cr_2O_3 = avg. 0.50 wt%). MgO content ranges between 12.5and 18.8 wt%; FeO shows the largest range variation (3.9 – 11.7 wt%) and MnO is usually undetected or little represented only in Fe-rich augite crystals (0.11 – 0.44 wt%). Mg# is in the range 66 – 89.

Compositional zoning, clearly observable in thin section, reflects an increasing from core to rim, in FeO TiO_2 and Al_2O_3 contents coupled with and MgO decrease.

4.1.2 Amphibole

Atomic proportions are based on an anhydrous basis per 23 oxigens and on different cation sum to account for minimum and maximum ferric estimate, according to Schumacher (1997). $Fe^{+2/+3}$ partitioning is given as an average of the minimum and the maximum ferric estimates (*Schumacher, 1997*). Amphibole nomenclature is according to Leake et al. (*1997*).

Analyses are reported in Appendix 2 - Table 2.2.

Calabrian dykes

Piani di Limina – Mammola dykes (LMA samples)

In LMA samples, amphibole is essentially represented by Tschermakite and Mg-Hastingsite (Fig. 4.3a, b). In the former, Mg# value is about 85, TiO_2, Na_2O and K_2O range between 3.0 – 3.5 wt.%, 2.4 - 2.9 wt.% and 0.7 – 0.8 wt.%, respectively.

Mg-Hastingsite is instead characterized by Mg# values and TiO_2 contents showing larger variation ranges (from 79 to 88 and from 2.8 – 4.0 wt.%, respectively). On the contrary, Na_2O and K_2O contents are constant (2.5 – 2.6 wt.%; 0.7 – 0.8 wt.%, respectively).

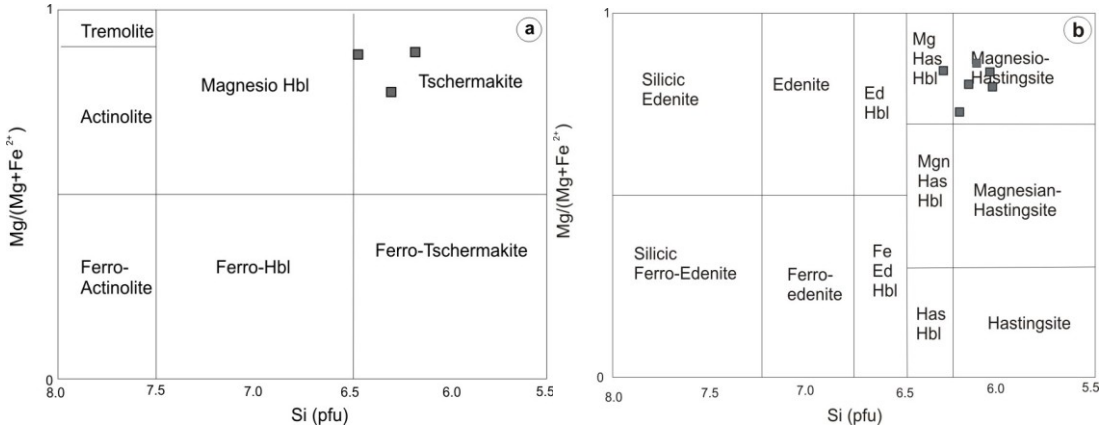

Fig. 4.3: Amphibole composition of LMA samples **a)** $Ca_B \geq 1.50$; ANa+AK<0.5; Ti<0.5 **b)** $Ca_B \geq 1.50$; ANa+AK ≥0.5; Ti<0.5; $Fe^3 > Al^{VI}$ (*Leake et al,. 1997*).

Foletti Valley dykes (F samples)

Amphibole in F samples is represented by Mg-hornblende and secondary actinolite (Fig. 4.4).

The former is characterized by Mg# values ranging from 70 to 90, TiO_2 contents between 0.00 and 2.17 wt. %, and Na_2O and K_2O contents up to 2.16 wt. % and 0.73 wt. %, respectively.

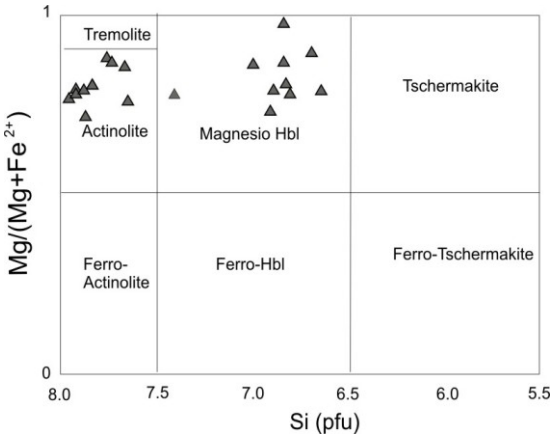

Fig. 4.4: Amphibole composition of F samples.

Antonimina dykes (A samples)

Amphiboles are represented by Tschermakite and Mg-hornblende (Fig. 4.5). The former shows Mg# values ranging from 64 to 88, Na_2O between 0.0 and 2.4 wt. % and K_2O between 0.0 and 0.7 wt. %. TiO_2 shows high contents up to 6.95 wt. %.
Mg-hornblende shows instead lower Mg# values (52 – 61) and TiO_2 contents (0.9 - 2.0 wt. %). Na_2O ranges between 1.7 and 2.0 wt. % and K_2O between 0.4 and 0.9 wt.%.
Secondary amphibole has actinolite–Fe-actinolite composition (Fig. 4.5).

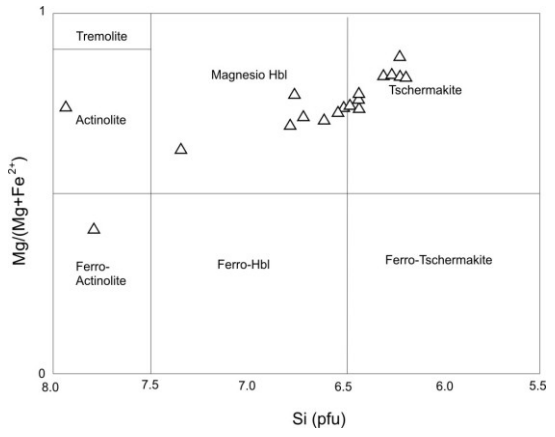

Fig. 4.5: Amphibole composition of A samples.

4.1.3 Feldspar

Atomic proportions are based on 32 oxigens and 20 cations.

Analyses are reported in Appendix 2 - Table 2.3.

Calabrian dykes

Feldspar grains of all Serre dykes are affected by a pervasive sericitization and saussuritization, particularly developed in VZ samples, for which several attempts to obtain reliable compositional data resulted unsuccessful.

On the whole, analyses have revealed a mainly secondary albitic composition for plagioclase from all studied samples (Fig. 4.6a, b, c, d), with a low to very low potassic component (up to 5.20%).

Only in the F samples, oligoclase grains have been detected ($An_{16.7\text{-}24.5}$).

Orthoclase is widespread in the matrix as interstitial phase in F (Or_{100}; Fig. 4.6b) and ST samples ($Or_{88.7\text{-}100.0}$; Fig. 4.6d) and, only in the first group, as subsolidus unmixing products in plagioclase crystals ($Or_{91.3\text{-}100.0}$).

Rare anorthoclase also occurs in LMA ($Ab_{64.5\text{-}78.1}$-$Or_{11.8\text{-}35.5}$; Fig. 4.14a), A ($Ab_{88.9}$-$Or_{9.1}$; Fig. 4.6c) and ST samples ($Ab_{84.4\text{-}85.4}$ – $Or_{14.0\text{-}15.2}$; Fig. 4.6d).

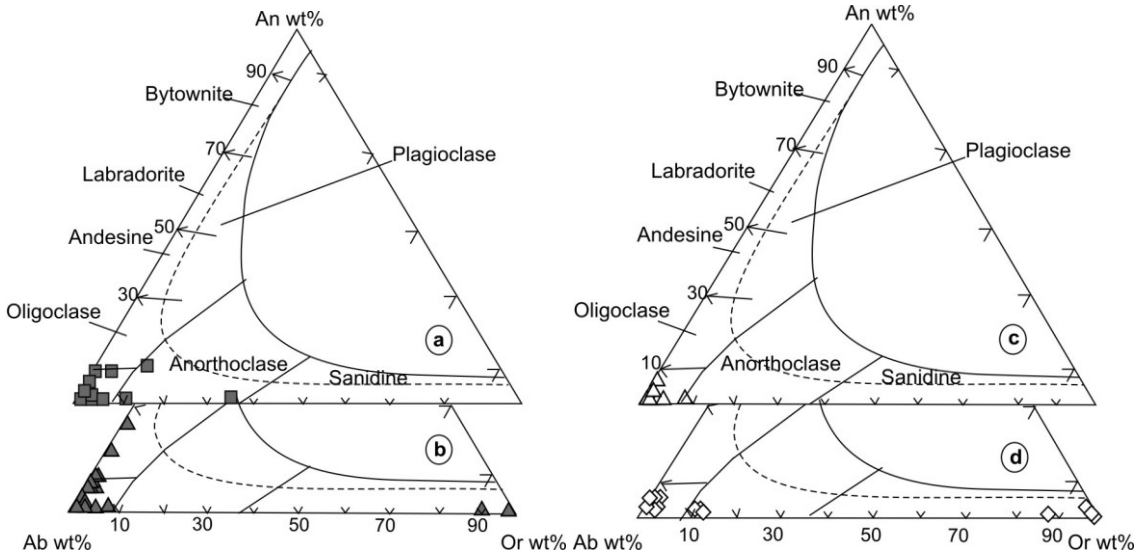

Fig. 4.6: Feldspar composition of Serre dykes. **a)** LMA-PDL samples; **b)** F samples; **c)** A samples; **d)** ST samples.

Sicilian dykes

Leonforte (VG samples)

Plagioclase of VG samples shows a secondary albitic composition ($Ab_{91.4\text{-}100.0}$; Fig. 4.7a), with a low potassic component (up to 5.7 wt. %). Additionally, rare anorthoclase ($Ab_{62.9\text{-}77.1}$-$Or_{20.0\text{-}32.7}$; Fig. 4.10a) and orthoclase (Or_{100}; Fig. 4.10a) crystals have been found. The latter occurs as interstitial phase or as products of subsolidus unmixing in plagioclase.

Plagioclase of BM samples commonly shows a composition ranging from labradorite to albite ($An_{69.8–0.5}$; Fig. 4.7b). Additionally, a normal compositional zoning has been detected from core to rim of some analyzed grain, reflecting a slight decrease in An (An_{core} = 69.3 –54.2; An_{rim} = 59.7 – 52.2).

Conversely, plagioclase of MA samples shows only a secondary albitic composition ($Ab_{94.0\text{-}100.0}$; Fig. 4.7c), with a low potassic component (up to 6.9 wt. %).

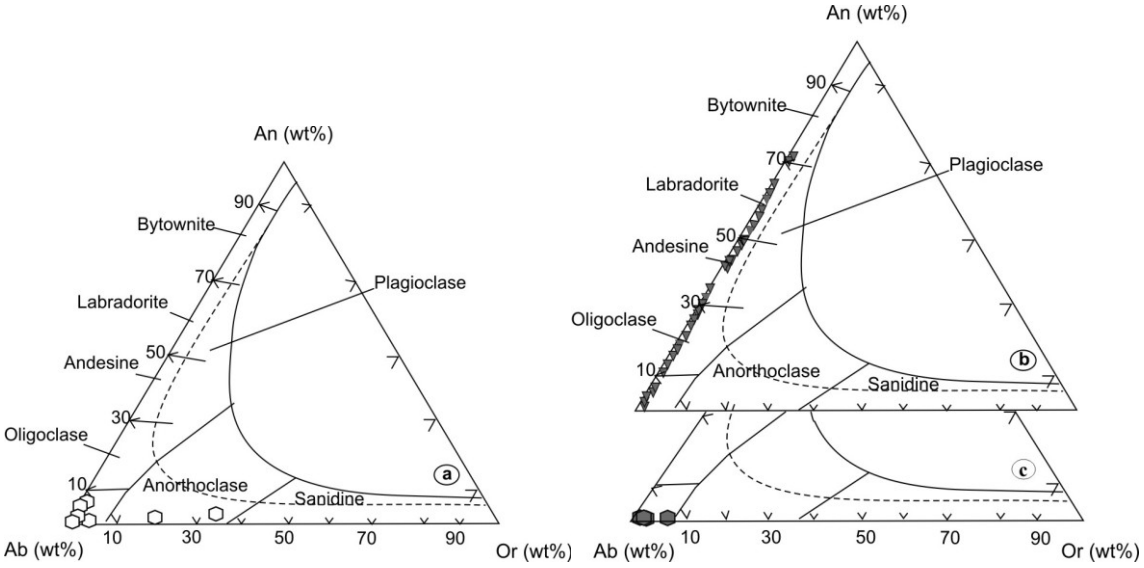

Fig. 4.7: Feldspar composition of Sicilian dykes: **a)** VG samples; **b)** BM samples; **c)** MA samples.

4.1.4 Biotite

Structural formulae are calculated on the basis of 24 oxigens and Fe^{+3}/Fe^{+2} repartition according to Dymek *(1983).*

Analyses are reported in Appendix 2 - Table 2.4

Leonforte dyke (VG samples)

Biotite is extensively chloritized. However, analyses have been performed in very rare preserved crystals. In many cases results indicate that the biotite primary compositions has been largely modified. Nevertheless, the analyzed compositions have been used to obtain a biotite classification taking into major account the composition of the freshest analyzed grains.

Analyses have revealed variable amounts of FeO (18.6-33.1 wt. %) and MgO (10.2-15.1 wt. %), that assigned to biotite an annite – phlogopite composition (Fig. 4.8). K_2O is highly variable (1.3 - 8.0 wt. %), TiO_2 ranges from 2.0 to 5.3 wt. % and Al_2O_3 from 12.7 to 14.7 wt. %.

In the FeO-MgO-Al_2O_3 diagram (*Abdel-Rahaman, 1993;* Fig. 4.9a), VG biotite compositions mainly fall in the calc-alkaline rock field. However, they show typical trends of alkaline biotite reflecting a gradual increasing in FeO contents with decreasing Al_2O_3 (*Abdel-Rahaman, 1993*). Additionally, in the MgO-FeO diagram (*Abdel-Rahaman, 1993;* Fig. 4.9b) biotite compositions clearly fall in the alkaline rock suites field.

The large variation range of FeO contents (19 – 33 wt. %) is another typical features of anorogenic and alkaline series.

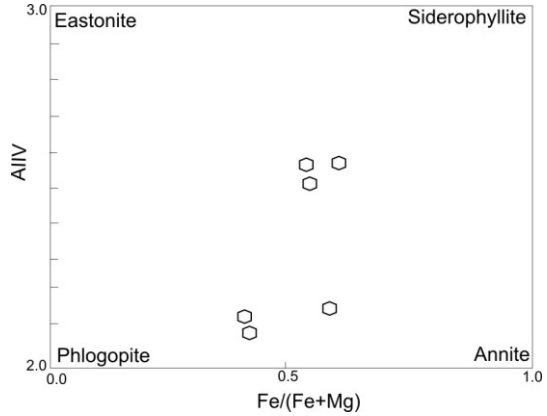

Fig. 4.8: Al^{IV} vs. Mg/Fe+Mg diagram for VG biotite composition.

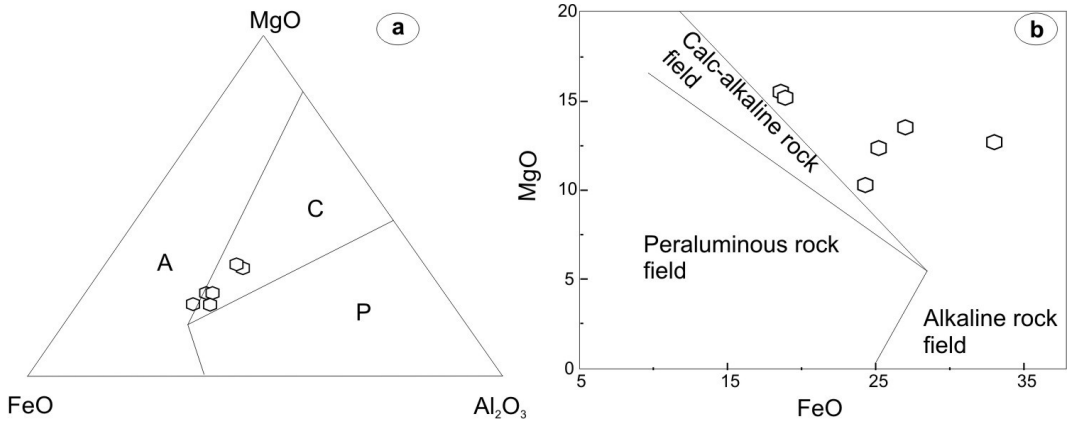

Fig. 4.9: a) FeO*-MgO-Al_2O_3 and **b)** Al_2O_3-FeO biotite discrimination diagrams for VG biotite. A field: anorogenic alkaline suites; P field: peraluminous suites; C field: calc-alkaline orogenic suites (*Abdel-Rahaman, 1993*).

4.1.5 White mica

Structural formulae has been calculated on the basis of 24 oxigens.
Analyses are reported in Appendix 2 - Table 2.5.

White mica has been recognized only in the Calabrian dykes of San Todaro (both groups I and II) and Villaggio Zomaro (VZ group) areas. However, textural and chemical criteria, as defined by Miller et al. (*1981*), suggest a magmatic origin only for some grains occurring in samples of the ST-II (muscovite-rich) group. In fact, numerous grains occurring in this sample group are characterized by a relatively large grain size

(up to ~500 μm) and usually well defined shapes, as indicated by the above cited authors for magmatic white mica.

Concerning the compositional criterion, Speer et al. (*1980*) and Miller et al. (*1981*) define magmatic white mica richer in Ti, Al and Na and poorer in Mg and Si than secondary one. However, the former authors indicate the Ti contents as the most diagnostic.

Texturally-defined primary muscovite of ST- group II samples is characterized by higher Na and Ti and lower Si and Mg contents than that considered secondary (Fig. 4.10), thus confirming their likely magmatic origin.

In addition, these grains generally show K_2O and Al_2O_3 ranging between 9.7 –10.4 wt. %, and 29.5 – 30.0 wt. %, respectively, relatively high TiO_2 contents (0.8-0.9 wt. %) and high MgO values(1.3 – 1.7 wt. %).

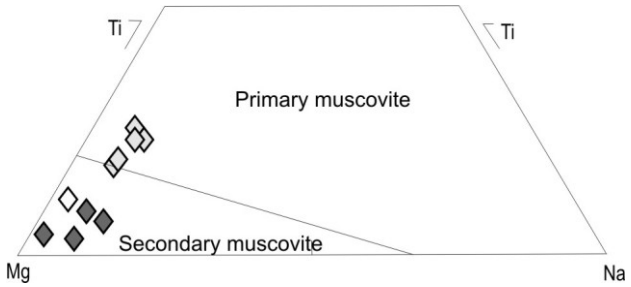

Fig. 4.10: Mg-Ti-Na discrimination diagram for white mica of ST-I and ST-II group (white and light grey rhombs, respectively) and VZ (dark grey rhombs) samples (*Miller et al., 1981*).

In the triangular diagram FeO-TiO_2-MgO (Fig. 4.11), Monier et al. (*1984*) recognize three types of muscovite: magmatic, late to post-magmatic and hydrothermal. The first one is typically rich in Ti and this content decreases with the typical magmatic evolution of a granite. The second one is richer in Fe than the hydrothermal type that, in turn, is richer in Ca and Mg.

Also according to this classification, muscovite of ST-group II could be considered magmatic, whereas those occurring in VZ samples would have a secondary origin.

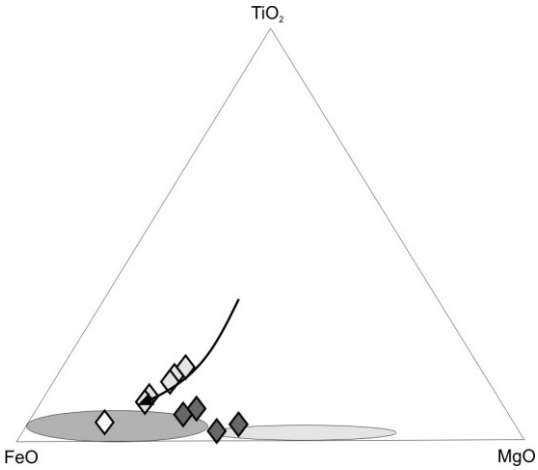

Fig. 4.11: Composition of ST-I, ST-II (white and light grey rhombs, respectively) and VZ (dark grey rhombs) white mica in the FeO-TiO_2-MgO (wt%) triangular diagram (*Monier et al., 1984*). Grey and light grey fields: late to post-magmatic muscovite and hydrothermal muscovite, respectively. Arrow represents the changing composition of the magmatic muscovite with the magmatic evolution of a granite.

4.1.6 Accessory minerals

Atomic proportions are based on 6 oxigens and 4 cations.

Ilmenite analyses are reported in Appendix 2 - Table 6.

Ilmenite, titanite and rutile represent the most abundant accessory minerals and they occur in almost all sampled dyke groups.

Ilmenite widely occurs in A and F dykes of Serre Massif. In the former group, it shows a variable composition ($Ilm_{69.7-78.4}$); TiO_2 contents ranges between 43.6 and 50.0 wt. % and FeO between 36.0 and 43.2 wt. %. MnO contents are very high (11.2 to 15.4 wt.%).

Ilmenite of F group ($Ilm_{88.8-90.8}$) shows higher FeO contents (42.2-47.5 wt.%) and comparable TiO_2 contents (45.1-45.7 wt.%). MnO ranges between 4 and 5 wt%.

Ilmenite of the Leonforte sill ($Ilm_{92.5-97.3}$) is characterized by FeO and TiO_2 contents ranging from 46.5to 48.9 wt. % and from 49.8 to 50.9 wt. %, respectively, and low MgO and MnO contents (0.29 - 1.61 wt. % and 0.82 - 3.11 wt. %, respectively).

In the Lercara area intrusions (BM and MA samples), ilmenite ($Ilm_{93.4-100.0}$, respectively) shows TiO_2 and FeO contents ranging from 53.1 to 62.9 wt. % and from 35.8 to 42.4 wt. %, respectively, very low MgO (0.55 - 1.32 wt.%) and no MnO.